Explorations of New Second-Order Nonlinear Optical Materials in the K-I-M-II -I-V-O Systems

ARTICLE *in* INORGANIC CHEMISTRY · MAY 2010

Impact Factor: 4.76 · DOI: 10.1021/ic100234e · Source: PubMed

6 AUTHORS, INCLUDING:

Xiang Xu
Chinese Academy of Sciences
58 PUBLICATIONS **667** CITATIONS
SEE PROFILE

Chuan-Fu Sun
University of Maryland, College Park
27 PUBLICATIONS **538** CITATIONS
SEE PROFILE

Jiang-Gao Mao
Chinese Academy of Sciences
283 PUBLICATIONS **5,895** CITATIONS
SEE PROFILE

Inorganic Chemistry
Article

Inorg. Chem. **2010**, *49*, 4599–4605 **4599**
DOI: 10.1021/ic100234e

Explorations of New Second-Order Nonlinear Optical Materials in the K^{I}-M^{II}-I^{V}-O Systems

Pei-Xin Li,[†,‡] Chun-Li Hu,[†] Xiang Xu,[†] Rui-Yao Wang, Chuan-Fu Sun,[†,‡] and Jiang-Gao Mao*[,†]

[†]*State Key Laboratory of Structural Chemistry, Fujian Institute of Research on the Structure of Matter, Chinese Academy of Sciences, Fuzhou 350002, P.R. China, and* [‡]*Graduate School of the Chinese Academy of Sciences, Beijing, 100039, P.R. China*

Received February 4, 2010

Explorations of new second-order nonlinear optical (NLO) materials in the K^{I}-M^{II}-I^{V}-O systems led to four novel mixed metal iodates, namely, $K_2M(IO_3)_4(H_2O)_2$ (M = Mn, Co, Zn, Mg). The four compounds are isostructural and crystallize in space group *I*2 which is in the chiral and polar crystal class 2. Their structure features zero-dimensional $\{M(IO_3)_4(H_2O)_2\}^{2-}$ anions that are separated by K^+ cations. The M(II) centers are ligated by two aqua ligands in trans fashion and four monodentate iodate anions. The K^+ cation is eight-coordinated by two iodate anions in bidentate chelating fashion and four other iodates in a unidentate fashion. Second harmonic generation (SHG) measurements indicate that $K_2Zn(IO_3)_4(H_2O)_2$ and $K_2Mg(IO_3)_4(H_2O)_2$ display moderate SHG responses that are approximately 2.3 and 1.4 times of KH_2PO_4 (KDP), respectively, and they are also phase-matchable. The SHG response of $K_2Co(IO_3)_4(H_2O)_2$ is much weaker (about 0.3 × KDP), and no obvious SHG signal was detected for $K_2Mn(IO_3)_4(H_2O)_2$. Results of optical property calculations for the Zn and Mg phases revealed SHG responses of approximately 5.3 and 4.7 times of KDP, respectively, the order of Zn > Mg is in good agreement with the experiment data.

Introduction

Noncentrosymmetric (NCS) compounds are of great interest because of their potential applications in many areas such as pyroelectricity, ferroelectricity, and especially second-order nonlinear optical (NLO) materials.[1,2] Several types of NLO materials based on metal oxides are well-known. For example, the most widely used such materials in ultraviolet and visible regions include borates such as β-BaB_2O_4 and LiB_3O_5 and phosphates such as KH_2PO_4 (KDP) and $KTiOPO_4$.[3] Such inorganic compounds with asymmetric or polar coordination geometries are likely to display NCS structures and exhibit good second harmonic generation (SHG) properties when these polar units are aligned in parallel manner. Recently, lots of attentions have been paid to use the anions with stereochemically active lone pair electrons as the structurally directing agents in the syntheses of second-order NLO materials. Anions with a nonbonding, but stereochemically active, pair of electrons have a tendency to form polar structures.[4] Some materials with good SHG properties have also been reported, such as $Se_2B_2O_7$ in which the lone pair cation Se(IV) was introduced into the borate system.[5] Also the combination of lone-pair cations with transition-metal ions with d^0 electronic configurations such as Mo^{6+} and W^{6+}, which are also susceptible to spin-orbit Jahn−Teller (SOJT) distortion, has proven to be an effective synthetic route for designing new SHG materials because of the additive polarization of both types of bonds when these polar second building units are properly aligned in their structures.[6]

Metal iodates also with a lone-pair cation have been reported to be able to display excellent NLO materials. Compared with other NLO materials, metal iodates such as α-$LiIO_4$ have been reported to show a wide transparency region, large

*To whom correspondence should be addressed. E-mail: mjg@fjirsm.ac.cn.

(1) (a) Lang, S. B.; Das-Gupta, D. K. In *Handbook of Advanced Electronic and Photonic Materials and Devices*; Nalwa, H. S., Ed.; Academic Press: San Francisco, 2001; Vol. *4*, pp 1−55. (b) Chen, C.; Liu, G. *Annu. Rev. Mater. Sci.* **1986**, *16*, 203. (c) Ok, K. M.; Halasyamani, P. S. *Chem. Soc. Rev.* **2006**, *35*, 710.

(2) Lines, M. E.; Glass, A. M. *Principles and Applications of Ferroelectrics and Related Materials*; Oxford University Press: Oxford, U.K., 1991.

(3) (a) Becker, P. *Adv. Mater.* **1998**, *10*, 979. (b) Chen, C.-T.; Wang, Y.-B.; Wu, B.-C.; Wu, K.-C.; Zeng, W.-L.; Yu, L.-H. *Nature* **1995**, *373*, 322. (c) Chen, C.-T.; Wu, B.-C.; Jiang, A.-D.; You, G.-M. *Sci. Sin., Ser. B.* **1985**, *28*, 235. (d) Hagerman, M. E.; Poeppelmeier, K. R. *Chem. Mater.* **1995**, *7*, 602.

(4) (a) Porter, Y.; Ok, K. M.; Bhuvanesh, N. S. P.; Halasyamani, P. S. *Chem. Mater.* **2001**, *13*, 1910. (b) Ok, K. M.; Bhuvanesh, N. S. P.; Halasyamani, P. S. *Inorg. Chem.* **2001**, *40*, 1978. (c) Kim, S. H.; Yeon, J.; Halasyamani, P. S. *Chem. Mater.* **2009**, *21*, 5335.

(5) Kong, F.; Huang, S.-P.; Sun, Z.-M.; Mao, J.-G.; Cheng, W.-D. *J. Am. Chem. Soc.* **2006**, *128*, 7750.

(6) (a) Halasyamani, P. S.; Poeppelmeier, K. R. *Chem. Mater.* **1998**, *10*, 2753. (b) Halasyamani, P. S. *Chem. Mater.* **2004**, *16*, 3586. (c) Ok, K. M.; Halasyamani, P. S. *Chem. Mater.* **2006**, *18*, 3176(8). (d) Chi, E. O.; Ok, K. M.; Porter, Y.; Halasyamani, P. S. *Chem. Mater.* **2006**, *18*, 2070. (e) Ra, H. S.; Ok, K. M.; Halasyamani, P. S. *J. Am. Chem. Soc.* **2003**, *125*, 7764.

(7) (a) Rosenzweig, A.; Morosin, B. *Acta Crystallogr.* **1966**, *20*, 758. (b) Phanon, D.; Gautier-Luneau, I. *Angew. Chem., Int. Ed.* **2007**, *46*, 8488. (c) Ok, K. M.; Halasyamani, P. S. *Angew. Chem., Int. Ed.* **2004**, *43*, 5489.

Published on Web 04/16/2010

second-harmonic generation (SHG) coefficients, high optical-damage thresholds, as well as good thermal stability.[7,8] So far, a large number of ternary metal iodates have been reported; the cations used cover alkali metal, alkaline earth metal, transition metal, lanthanide metal, post-transition metal main group elements such as indium and gallium, as well as actinide metal ions such as U^{6+} and Th^{4+}.[7−11] A few of them exhibit excellent SHG properties such as NaI_3O_8, $In(IO_3)_3$, $Ga(IO_3)_3$, $La(IO_3)_3$, $Cs_2I_4O_{11}$.[7−10] The quaternary metal iodates such as $AMoO_3(IO_3)$ (A = K, Rb, Cs),[12a] $Li_2Ti(IO_3)_6$,[12f] and $BaNbO(IO_3)_5$[12g] with the combination of the stereochemically active lone pair electrons and d^0 transition metals also display excellent SHG properties.[12]

A few other quaternary mixed metal iodates have also been studied, including $K_3In(IO_3)_6$, $Mn_{1-x}Zn_x(IO_3)_2$, $ZnPb(IO_3)_6(H_2O)_6$, $K_2Ge(IO_3)_6$, $RbLi_2(IO_3)_3$, $NaY(IO_3)_4$, $K_3Am_3(IO_3)_{12}\cdot HIO_3$ and a series of $Ln_3Pb_3(IO_3)_{13}(\mu_3\text{-O})$ (Ln = La−Nd).[13] Among them, α-$K_3In(IO_3)_6$ and $La_3Pb_3(IO_3)_{13}(\mu_3\text{-O})$ show moderate SHG response.

We are especially interested in the quarternary mixed metal iodates in the K-M(II)-IO_3 system in which the divalent M^{2+} ions are in the octahedral geometry and the adjacent $I(V)O_3$ groups are apart as far as possible from each other by the space requirement of the lone pair electrons. So far, no such compounds have been reported yet. We hope to understand the role of the nature of the divalent metal ion such as the ionic radius and the electronic configuration on the structures and SHG properties of these compounds. Our explorations in these systems afforded four isomorphic polar compounds, namely, $K_2M(IO_3)_4(H_2O)_2$ (M = Mn, Co, Zn, Mg), among which, the Zn and Mg phases display moderate SHG responses that are approximately 2.3 and 1.4 times of KDP, respectively. Here, we report their syntheses, crystal structures, and optical properties.

Experimental Section

Materials and Instrumentation. All of the chemicals were analytically pure from commercial sources and used without further purification: KIO_3 (AR, YuHuanShengHua Reagent Co.), $MgCl_2\cdot 6(H_2O)$ (AR, Shanghai ZhenXing Reagent Co.), $Zn(Ac)_2$ (AR, Shanghai Chemical Reagent Co.), $CoCl_2\cdot 6(H_2O)$ (AR, Shanghai Chemical Reagent Co.), $Mn(Ac)_2\cdot 4H_2O$ (AR JingShanXinTa Reagent Co.), $NH_4H_2(PO_4)$ (AR, Shanghai Chemical Reagent Co.). Elemental analyses for K, M, I were performed with a JEOL-6700F scan electronic microscope. X-ray diffraction (XRD) powder patterns were collected on a XPERT-MPD $\theta-2\theta$ diffractometer. IR spectra were recorded on a Magna 750 FT-IR spectrometer as KBr pellets in the range of 4000−400 cm^{-1}. Thermogravimetric analyses (TGA) were carried out with a NETZSCH STA 449C unit, at a heating rate of 15 °C/min under a nitrogen atmosphere. Optical diffuse reflectance spectra were measured at room temperature with a PE Lambda 900 UV−visible spectrophotometer. The instrument was equipped with an integrating sphere and controlled by a personal computer. $BaSO_4$ plate was used as a standard (100% reflectance). The absorption spectrum was calculated from the reflectance spectrum using the Kubelka−Munk function: $\alpha/S = (1-R)^2/2R$,[14] where α is the absorption coefficient, S is the scattering coefficient which is practically wavelength independent when the particle size is larger than 5 μm, and R is the reflectance. The measurements of the powder frequency-doubling effect were carried out on the sieved (80−100 mesh) powder samples of $K_2M(IO_3)_4(H_2O)_2$ (M = Mn, Co, Zn, Mg) by means of the modified method of Kurtz and Perry.[15] The fundamental wavelength is 1064 nm generated by a Q-switched Nd:YAG laser. The SHG wavelength is 532 nm. KDP was used as reference to assume the effect. SHG efficiency has been shown to depend strongly on particle size, thus samples of KDP as well as those of the Zn and Mg compounds were ground and sieved into several distinct particle size ranges (0−25, 25−44, 44−53, 53−74, 74−105, 105−149, 149−210, 210−250, 250−325 μm). All of the samples were placed in separate capillary tubes. No index-matching fluid was used in any of the experiments.

Synthesis of $K_2Mn(IO_3)_4(H_2O)_2$. A mixture of KIO_3 (0.2166 g, 1.01 mmol), $Mn(Ac)_2\cdot 4H_2O$ (0.0529 g, 0.22 mmol), and $NH_4H_2PO_4$ in 10 mL of distilled water was sealed in an autoclave equipped with a Teflon linear (25 mL) and then heated at 100 °C for 5 days, followed by cooling at 0.04 °C/min to room temperature. The initial and final pH values of the reaction media are both close to 5.0. Light pink single crystals of $K_2Mn(IO_3)_4(H_2O)_2$ were collected in a very low yield (< 20.0 mg). Although $NH_4H_2PO_4$ is not present in the final products, however, the compound could not be isolated in absence of $NH_4H_2PO_4$. Also two other impurity phases, $Mn_3(PO_4)_2$ and KIO_3, were found in the reaction products. Attempts to improve the yield by changing reaction conditions such as temperature, molar ratio of the starting materials, and different metal sources such as $MnCl_2$ also were tried but were unsuccessful. IR (KBr, cm^{-1}): 3030 br, 760 vs, 726 s. Microprobe analyses on several single crystals of $K_2Mn(IO_3)_4(H_2O)_2$ gave an average Mn/K/I molar ratio of 1:2.1:3.9, which is in agreement with that obtained from single crystal X-ray diffraction studies.

(8) (a) Phanon, D.; Gautier-Luneau, I. *J. Mater. Chem.* **2007**, *17*, 1123. (b) Ok, K. M.; Halasyamani, P. S. *Inorg. Chem.* **2005**, *44*, 9353.
(9) (a) Ngo, N.; Kalachnikova, K.; Assefa, Z.; Haire, R. G.; Sykora, R. E. *J. Solid State Chem.* **2006**, *179*, 3824. (b) Phanon, D.; Bentria, B.; Benbertal, D.; Mosset, A.; Gautier-Luneau, I. *Solid State Sci.* **2006**, *8*, 1466. (c) Chen, X.; Xue, H.; Chang, X.; Zang, H.; Xiao, W. *J. Alloys Compd.* **2005**, *398*, 173. (d) Assefa, Z.; Ling, J.; Haire, R. G.; Albrecht-Schmitt, T. E.; Sykora, R. E. *J. Solid State Chem.* **2006**, *179*, 3653. (e) Sykora, R. E.; Khalifah, P.; Assefa, Z.; Albrecht-Schmitt, T. E.; Haire, R. G. *J. Solid State Chem.* **2008**, *181*, 1867. (f) Douglas, P.; Hector, A. L.; Levason, W.; Light, M. E.; Matthews, M. L.; Webster, M. Z. *Anorg. Allg. Chem.* **2004**, *630*, 479. (g) Hector, A. L.; Henderson, S. J.; Levason, W.; Webster, M. Z. *Anorg. Allg. Chem.* **2002**, *628*, 198.
(10) (a) Bean, A. C.; Campana, C. F.; Kwon, O.; Albrecht-Schmitt, T. E. *J. Am. Chem. Soc.* **2001**, *123*, 8806. (b) Bean, A. C.; Peper, S. M.; Albrecht-Schmitt, T. E. *Chem. Mater.* **2001**, *13*, 1266. (c) Ling, J.; Albrecht-Schmitt, T. E. *Inorg. Chem.* **2007**, *46*, 346. (d) Sykora, R. E.; Wells, D. M.; Albrecht-Schmitt, T. E. *Inorg. Chem.* **2002**, *41*, 2304. (e) Bray, T. H.; Beitz, J. V.; Bean, A. C.; Yu, Y.; Albrecht-Schmitt, T. E. *Inorg. Chem.* **2006**, *45*, 8251. (f) Bean, A. C.; Ruf, M.; Albrecht-Schmitt, T. E. *Inorg. Chem.* **2001**, *40*, 3959.
(11) (a) Sykora, R. E.; McDaniel, S. M.; Wells, D. M.; Albrecht-Schmitt, T. E. *Inorg. Chem.* **2002**, *41*, 5126. (b) Bean, A. C.; Xu, Y.; Danis, J. A.; Albrecht-Schmitt, T. E. *Inorg. Chem.* **2002**, *41*, 6775. (c) Sykora, R. E.; Bean, A. C.; Scott, B. L.; Runde, W.; Albrecht-Schmitt, T. E. *J. Solid State Chem.* **2004**, *177*, 725. (d) Sullens, T. A.; Almond, P. M.; Byrd, J. A.; Beitz, J. V.; Bray, T. H.; Albrecht-Schmitt, T. E. *J. Solid State Chem.* **2006**, *179*, 1192. (e) Bean, A. C.; Albrecht-Schmitt, T. E. *J. Solid State Chem.* **2001**, *161*, 416.
(12) (a) Sykora, R. E.; Ok, K. M.; Halasyamani, P. S.; Albrecht-Schmitt, T. E. *J. Am. Chem. Soc.* **2002**, *124*, 1951. (b) Shehee, T. C.; Sykora, R. E.; Ok, K. M.; Halasyamani, P. S.; Albrecht-Schmitt, T. E. *Inorg. Chem.* **2003**, *42*, 457. (c) Sykora, R. E.; Wells, D. M.; Albrecht-Schmitt, T. E. *Inorg. Chem.* **2002**, *41*, 2697. (d) Sykora, R. E.; Ok, K. M.; Halasyamani, P. S.; Wells, D. M.; Albrecht-Schmitt, T. E. *Chem. Mater.* **2002**, *14*, 2741. (e) Chang, H. Y.; Kim, S. H.; Halasyamani, P. S.; Ok, K. M. *J. Am. Chem. Soc.* **2009**, *131*, 2426. (f) Ok, K. M.; Halasyamani, P. S. *Inorg. Chem.* **2005**, *44*, 2263. (g) Sun, Ch.-F.; Hu, Ch.-L.; Xu, X.; Ling, J.-B.; Hu, T.; Kong, F.; Long, X.-F.; Mao, J.-G. *J. Am. Chem. Soc.* **2009**, *131*, 9486.
(13) (a) Zloczysti, S.; Hartl, H.; Frydrych, R. *Acta Crysrallogr., Sect. B.* **1976**, *32*, 753–758. (b) Schellhaas, F.; Hartl, H.; Frydrych, R. *Acta Crysrallogr., Sect. B.* **1972**, *28*, 2834–2838. (c) Kalinin, V. R.; Ilyukhin, V. V.; Belov, N. V. *Coord. Chem.* (*U.S.S.R.*) **1978**, *4*, 444–447. (d) *Acta Chem. Scand.* **1966**, *20*, 2886−2888. (e) *Acta Chem. Scand.* **1965**, *19*, 875−878. (f) Currie, D. B.; Levason, W.; Oldroyd, R. D.; Weller, M. T. *J. Mater. Chem.* **1993**, *3*, 447. (g) Hu, T.; Qin, L.; Kong, F.; Zhou, Y.; Mao, J.-G. *Inorg. Chem.* **2009**, *48*, 2193.
(14) (a) Kubelka, P.; Munk, F. Z. *Tech. Phys.* **1931**, *12*, 593. (b) Wendlandt, W. M.; Hecht, H. G. *Reflectance Spectroscopy*; Interscience: New York, 1966.
(15) Kurtz, S. W.; Perry, T. T. *J. Appl. Phys.* **1968**, *39*, 3798.

Table 1. Crystal Data and Structural Refinements for $K_2M(IO_3)_4(H_2O)_2$ (M = Mn, Co, Zn, Mg)

compound	$K_2Mn(IO_3)_4(H_2O)_2$	$K_2Co(IO_3)_4(H_2O)_2$	$K_2Zn(IO_3)_4(H_2O)_2$	$K_2Mg(IO_3)_4(H_2O)_2$
formula	$K_2MnI_4O_{14}H_4$	$K_2CoI_4O_{14}H_4$	$K_2ZnI_4O_{14}H_4$	$K_2MgI_4O_{14}H_4$
Fw	868.77	872.76	879.20	838.14
space group	*I*2 (No. 5)	*I*2 (No. 5)	*I*2 (No. 5)	*I*2 (No. 5)
a/Å	8.356(5)	8.285(7)	8.289(4)	8.305(9)
b/Å	7.761(2)	7.738(3)	7.733(8)	7.760(8)
c/Å	11.166(4)	11.043(6)	11.08(1)	11.10(1)
β/deg	90.09(3)	90.06(5)	90.12(3)	90.01(1)
V/Å^3	724.1(5)	708.0(7)	710 (1)	716(1)
Z	2	2	2	2
D_c/g.cm^{-3}	3.985	4.094	4.111	3.891
μ(Mo−Kα)/mm^{-1}	10.081	10.589	11.078	9.405
Goodness-of-fit on F^2	1.020	1.077	1.066	1.056
Flack factor			0.04(4)	0.05(8)
R1, wR2 [$I > 2\sigma(I)$][a]	0.0139, 0.0313	0.0355, 0.0722	0.0200, 0.0453	0.0674, 0.1760
R1, wR2 (all data)	0.0140, 0.0314	0.0367, 0.0736	0.0200, 0.0453	0.0697, 0.1802

[a] $R1 = \sum||F_o| - |F_c||/\sum|F_o|$, $wR2 = \{\sum w(F_o^2 - F_c^2)^2/\sum w(F_o^2)^2\}^{1/2}$.

Syntheses of $K_2M(IO_3)_4(H_2O)_2$ (M = Co, Zn, Mg). The three compounds were hydrothermally synthesized by the reactions of a mixture of hexahydrated metal chloride (for **Co** and **Mg** compounds) or zinc(II) acetate and potassium iodate in 10 mL of distilled water, which was sealed in an autoclave equipped with a Teflon linear (25 mL) at 100 °C for 5 days, followed by cooling at a rate of 0.04 °C/min to room temperature. The K/M molar ratios are equal to 4: 1 for the three compounds. The initial and final pH values of the reaction media are close to 5.0 for all three compounds. Single crystals of the three compounds were collected in a yield of 33.4%, 50%, 70%, respectively (based on M). IR data (KBr, cm^{-1}) for the **Co** compound: 3055 br, 801 m, 762 vs, 721 m, IR data (KBr, cm^{-1}) for the **Zn** compound: 3010 br, 2320 w, 802 m, 765 vs, 722 s. IR data (KBr, cm^{-1}) for the **Mg** compound: 3069 br, 801−782 vs, 721 m. Microprobe analyses on several single crystals of each compound gave average M/K/I molar ratios of 1:1.8:4, 1:2.1:4 and 1:1.9:4 for the **Co**, **Zn**, and **Mg** compounds, respectively, which are in good agreement with those obtained from single crystal X-ray diffraction studies. The powder XRD patterns for $K_2M(IO_3)_4(H_2O)_2$ (M = Co, Zn, Mg) are in good agreement with those simulated from the single-crystal data, hence they are pure phases (See Supporting Information, Figure S1).

Single-Crystal Structure Determination. Data collections for $K_2M(IO_3)_4(H_2O)_2$ (M = Mn, Co, Zn, Mg) were performed on a Rigaku Mercury CCD diffractometer equipped with a graphite-monochromated Mo Kα radiation (λ = 0.71073 Å) at 293(2) K. All four data sets were corrected for Lorentz and polarization factors as well as for absorption by Multiscan method.[16a] All four structures were solved by the direct methods and refined by full-matrix least-squares fitting on F^2 by SHELX-97.[16b] The data sets of the **Mn**, **Co**, **Zn** compounds gave high R1 values (> 10%) before the twin problem was solved (monoclinic emulate orthorhombic because of β angles close to 90° as well as racemic twining for **Co** and **Mn** compounds).[17] For **Zn** compound, the reflections from the two domain components were used for the structural solution and refinements with the twin law of 1 0 0 0 −1 0 0 0 1, and the basf value is refined to be 0.40942. For **Mn** and **Co**, the twin law of 1 0 0 0 −1 0 0 0 1 −4 was applied, and the three basf parameters are refined to 0.72171, 0.09150, and 0.12023 for the **Mn** compound, and 0.30823, 0.16451, and 0.19532 for the **Co** compound. These treatments led to satisfactory R1 values of 0.0139, 0.0355 and 0.0200, respectively for the **Mn**, **Co** and **Zn** compounds. All non-hydrogen atoms were refined with anisotropic thermal parameters. The hydrogen atoms of the aqua ligands were located at geometrically calculated positions and refined with isotropic thermal parameters. Crystallographic data and structural refinements for the four compounds are summarized in Table 1. Important bond distances are listed in Table 2. More details on the crystallographic studies as well as atomic displacement parameters are given as Supporting Information.

Further details of the crystal structure studies can be obtained from the Fachinformationszentrum Karlsruhe, 76344 Eggenstein-Leopoldshafen, Germany (Fax: (49) 7247808666; e-mail: crysdata@fiz-karlsruhe.de), on quoting the depository numbers CSD 421244, 421243, 421242, and 421245.

Computational Descriptions. The band structure, density of states (DOS), and optical property calculations were carried out by using the total-energy code of CASTEP.[18] The total energy was calculated within the framework of nonlocal gradient-corrected approximations.[19] The interactions between the ionic cores and the electrons were described by the norm-conserving pseudopotentials.[20] The following orbital electrons were treated as valence electrons: K-3s^{2}3p^{6}4s^1, Mg-3s^2, Zn-3d^{10}4s^2, I-5s^{2}5p^5, and O-2s^{2}2p^4. The number of plane waves included in the basis was determined by a cutoff energy of 600 and 500 eV, and the numerical integration of the Brillouin zone was performed using a 3 × 3 × 2 and 3 × 3 × 2 Monkhorst-Pack k-point sampling for the **Zn** and **Mg** compounds, respectively. The other calculation parameters and convergent criteria were the default values of the CASTEP code.[18]

The calculations of linear optical properties in terms of the complex dielectric function $\varepsilon(\omega) = \varepsilon_1(\omega) + i\varepsilon_2(\omega)$ were performed. The imaginary part of the dielectric function ε_2 is given in the following equation.[21]

$$\varepsilon_2^{ij}(\omega) = \frac{8\pi^2\hbar^2e^2}{m^2V}\sum_k\sum_{cv}(f_c - f_v)\frac{p_{cv}^i(k)p_{vc}^j(k)}{E_{vc}^2}\delta[E_c(k) - E_v(k) - \hbar\omega] \quad (1)$$

The f_c and f_v represent the Fermi distribution functions of the conduction bands (CBs) and valence bands (VBs), respectively. The term $p_{cv}^i(k)$ denotes the momentum matrix element transition from the energy level c of the CB to the level v of the VB at a certain k point in the Brillouin zones and V is the volume of the

(16) (a) *CrystalClear*, version. 1.3.5; Rigaku Corp.: Woodlands, TX, 1999. (b) Sheldrick, G. M. *SHELXTL, Crystallographic Software Package, SHELXTL, Version 5.1*; Bruker-AXS: Madison, WI, 1998.

(17) Flack, H. D. *Acta Crystallogr.* **1983**, *A39*, 876–881.

(18) (a) Segall, M. D.; Lindan, P. J. D.; Probert, M. J.; Pickard, C. J.; Hasnip, P. J.; Clark, S. J.; Payne, M. C. *J. Phys.: Condens. Matter.* **2002**, *14*, 2717. (b) Milman, V.; Winkler, B.; White, J. A.; Pickard, C. J.; Payne, M. C.; Akhmatskaya, E. V.; Nobes, R. H. *Int. J. Quantum Chem.* **2000**, *77*, 895.

(19) Perdew, J. P.; Burke, K.; Ernzerhof, M. *Phys. Rev. Lett.* **1996**, *77*, 3865.

(20) Lin, J. S.; Qteish, A.; Payne, M. C.; Heine, V. *Phys. Rev. B.* **1993**, *47*, 4174.

(21) Bassani, F.; Parravicini, G. P. *Electronic States and Optical Transitions In Solids*; Pergamon Press Ltd.: Oxford, 1975; pp 149−154.

Table 2. Selected Bond Lengths (Å) for $K_2M(IO_3)_4(H_2O)_2$ (M = Mn, Co, Zn, Mg)[a]

	compound Mn	compound Co	compound Zn	compound Mg
K(1)−O(1)#1	2.773(5)	2.73(1)	2.743(9)	2.76(1)
K(1)−O(1)#2	2.773(5)	2.73(1)	2.743(9)	2.76(1)
K(1)−O(6)#3	2.828(4)	2.80(1)	2.787(7)	2.81(1)
K(1)−O(6)#4	2.828(4)	2.80(1)	2.787(7)	2.81(1)
K(1)−O(4)	2.825(4)	2.81(1)	2.808(6)	2.825(1)
K(1)−O(4)#5	2.825(4)	2.81(1)	2.808(6)	2.825(1)
K(1)−O(3)#5	2.919(4)	2.93(1)	2.934(6)	2.92(1)
K(1)−O(3)	2.919(4)	2.93(1)	2.934(6)	2.92(1)
K(2)−O(1)#2	2.744(4)	2.72(2)	2.715(8)	2.70(1)
K(2)−O(1)#1	2.744(4)	2.72(2)	2.715(8)	2.70(1)
K(2)−O(6)#7	2.754(4)	2.72(1)	2.726(7)	2.72(1)
K(2)−O(6)#8	2.754(4)	2.72(1)	2.726(7)	2.72(1)
K(2)−O(5)#5	2.921(4)	2.88(1)	2.903(7)	2.90(1)
K(2)−O(5)	2.921(4)	2.88(1)	2.903(7)	2.90(1)
K(2)−O(2)#2	3.172(4)	3.18(1)	3.180(6)	3.20(1)
K(2)−O(2)#1	3.172(4)	3.18(1)	3.180(6)	3.20(1)
M(1)−O(2W)	2.099(5)	2.03(1)	2.018(9)	2.04(2)
M(1)−O(1W)	2.134(6)	2.11(1)	2.07(1)	2.05 (2)
M(1)−O(2)#7	2.170(3)	2.110(9)	2.113(6)	2.12(1)
M(1)−O(2)#2	2.170(3)	2.110(9)	2.113(6)	2.12(1)
M(1)−O(5)#10	2.236(4)	2.16(1)	2.204(6)	2.20(1)
M(1)−O(5)	2.236(4)	2.16(1)	2.204(6)	2.20(1)
I(1)−O(3)	1.797(3)	1.782(9)	1.790(6)	1.80(1)
I(1)−O(1)	1.802(3)	1.801(8)	1.802(5)	1.811(8)
I(1)−O(2)	1.830(4)	1.81(1)	1.842(6)	1.82(1)
I(2)−O(6)	1.804(3)	1.79(1)	1.810(5)	1.811(8)
I(2)−O(4)	1.814(4)	1.799(8)	1.814(7)	1.82(1)
I(2)−O(5)	1.821(4)	1.88(1)	1.819(7)	1.84(1)

[a] Symmetry transformations used to generate equivalent atoms: #1 $-x-1/2$, $y+1/2$, $-z+1/2$; #2 $x+1/2$, $y+1/2$, $z-1/2$; #3 $x-1/2$, $y-1/2$, $z-1/2$; #4 $-x+1/2$, $y-1/2$, $-z+1/2$; #5 $-x, y, -z$; #6 $x, y-1, z$; #7 $-x+1/2$, $y+1/2$, $-z+1/2$; #8 $x-1/2$, $y+1/2$, $z-1/2$; #9 $x, y+1, z$; #10 $-x+1, y, -z$.

unit cell. The m, e, and $\hbar$ are the electron mass, charge and Plank's constant, respectively.

The second-order optical properties were calculated based on momentum-gauge formalism with the minimal-coupling interaction Hamiltonian and within the independent-particle approximation.[22,23] The imaginary part of the frequency-dependent second-order susceptibility $\chi^{(2)}(2\omega,\omega,\omega)$ is obtained from the electronic band structures by using the expressions already given elsewhere.[24−26] Then we use the Kramers−Kronig relations, as required by causality, to obtain the real part

$$\chi'^{(2)}(-2\omega,\omega,\omega) = \frac{2}{\pi}P\int_0^\infty d\omega' \frac{\omega'\chi''^{(2)}(2\omega',\omega',\omega')}{\omega'^2-\omega^2} \quad (2)$$

In the present study, the δ function in the expressions for $\chi^{(2)}(2\omega,\omega,\omega)$ is approximated by a Gaussian function with Γ = 0.2 eV. Furthermore, to ensure that the real part calculated via the Kramers−Kronig transformation (eq 2) is reliable, at least 300 empty bands were used in SHG calculation. In addition, because DFT-GGA fails to correctly predict the CB energies, the CB energy should be corrected by adding a scissor operator; meanwhile, the momentum matrix elements were also renormalized correspondingly.[27]

(22) Ghahramani, E.; Moss, D. J.; Sipe, J. E. *Phys. Rev. B.* **1991**, *43*, 8990.
(23) Ghahramani, E.; Moss, D. J.; Sipe, J. E. *Phys. Rev. Lett.* **1990**, *64*, 2815.
(24) Duan, C.-G.; Li, J.; Gu, Z.-Q.; Wang, D.-S. *Phys. Rev. B.* **1999**, *60*, 9435.
(25) Guo, G.-Y.; Chu, K.-C.; Wang, D.-S.; Duan, C.-G. *Phys. Rev. B.* **2004**, *69*, 205416.
(26) (a) Guo, G.-Y.; Lin, J.-C. *Phys. Rev. B.* **2005**, *72*, 075416. (b) Guo, G.-Y.; Lin, J.-C. *Phys. Rev. B.* **2008**, *77*, 049901.
(27) (a) Godby, R.-W.; Schluther, M.; Sham, L. J. *Phys. Rev. B.* **1987**, *36*, 6497. (b) Okoye, C. M. I. *J. Phys.: Condens. Matter* **2003**, *15*, 5945. (c) Terki, R.; Bertrand, G.; Aourag, H. *Microelectron. Eng.* **2005**, *81*, 514. (d) Jiang, H.-L.; Kong, F.; Mao, J.-G. *J. Solid State Chem.* **2007**, *180*, 1764.

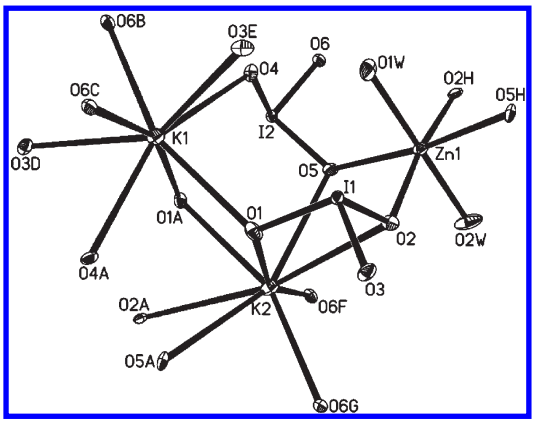

Figure 1. ORTEP representation of the selected unit in $K_2Zn(IO_3)_4(H_2O)_2$. The thermal ellipsoids are drawn at the 50% probability level. Symmetry codes for the generated atoms: (a) $1-x, y, -z$ (b) $x-1/2, y-1/2, z-1/2$ (c) $-x+1/2, y-1/2, -z+1/2$ (d) $-x+1/2, y-1/2, -z-1/2$ (e) $x-1/2, y-1/2, z+1/2$ (f) $-x+1/2, y+1/2, -z+1/2$ (g) $x-1/2, y+1/2, z-1/2$ (h) $-x+1, y, -z$.

Results and Discussion

Hydrothermal synthesis is an effective method for the preparation of metal iodates. The reactions of transition metal salts or magnesium chloride and potassium iodates, afforded a series of novel quaternary mixed metal iodates, namely, $K_2M(IO_3)_4(H_2O)_2$ (M = Mn, Co, Zn, Mg). These compounds are isostructural, and their structures feature a zero-dimensional (0D) anion stucture; hence, only the structure of the Zn compound will be discussed in detail as a representative.

The asymmetric unit of $K_2Zn(IO_3)_4(H_2O)_2$ contains one zinc(II) ion, two potassium(I) cations, two iodate anions, and two aqua ligands. The zinc(II) and potasium(I) ions and aqua ligands are on sites of 2-fold axis, whereas the remaining atoms occupy general positions. As show in Figure 1, the Zn^{2+} ion is octahedrally coordinated by four iodate anions in a unidentate fashion and two aqua ligands, with the Zn−O bond distances in the range of 2.018(9)−2.204(6) Å (Table 2); hence, the ZnO_6 octahedron is slightly distorted. Each I^{5+} cation is bonded to three oxygen atoms in a trigonal pyramidal coordination environment as a result of its stereoactive lone pair; the I−O distances range from 1.790(6)−1.842(6) Å. The K atom is eight-coordinated by two iodates anions in bidentate chelated fashion and four iodates in a unidentate fashion. The K−O bond distances are in range of 2.715(8)−3.180(6) Å; these bond distances are comparable to those reported for other potassium(I) iodates.[8] According to the bond valence analyses,[28] the zinc atoms are +2 and the iodate atoms are +5 in charge, and the calculated total bond valences are 2.06, 5.07, and 4.92 for Zn(1), I(1), and I(2), respectively.

It is noticed that two water ligands and four iodates are in *trans* fashion around the metal center, the polarizations of the $I(2)O_3^-$ groups almost cancel each other whereas those of $I(1)O_3^-$ groups are aligned in a parallel manner, and the latter produces a net dipole moment along the *b*-axis (see Figure 2a). Neighboring 0D $Zn(IO_3)_4(H_2O)_2^{2-}$ anions are packed in such a way that they produce a large macroscopic dipole moment along the *b*-axis (see Supporting Information, Figure S2) as required by the space group symmetry, thereby

(28) Brese, N. E.; O'Keeffe, M. *Acta Crystallogr.* **1991**, *B47*, 192.

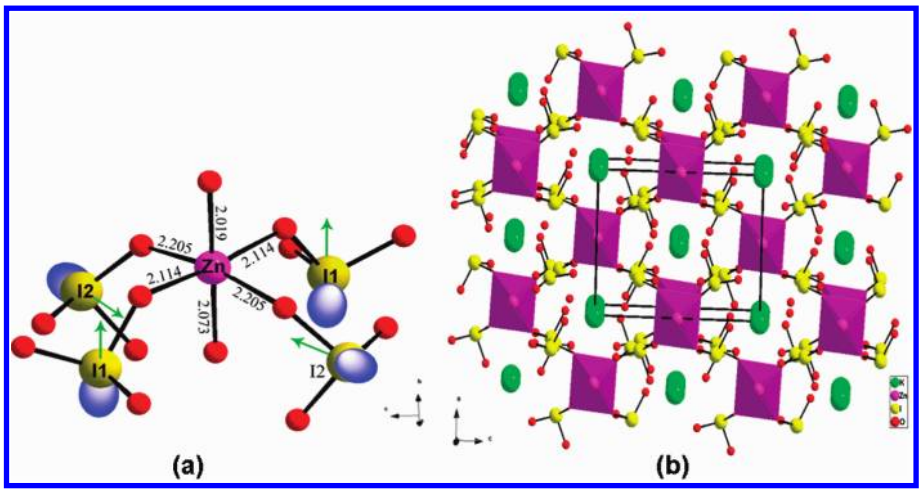

Figure 2. 0D unit of $[Zn(IO_3)_4(H_2O)_2]^{2-}$ anions, lone pairs (blue ellipsoids), and local moments (green arrows) in $K_2Zn(IO_3)_4(H_2O)_2$ (a), and view of the structure of $K_2Zn(IO_3)_4(H_2O)_2$ along *b* axis (b). K, Zn, I, and O atoms are represented by green, pink, yellow, and red circles, respectively.

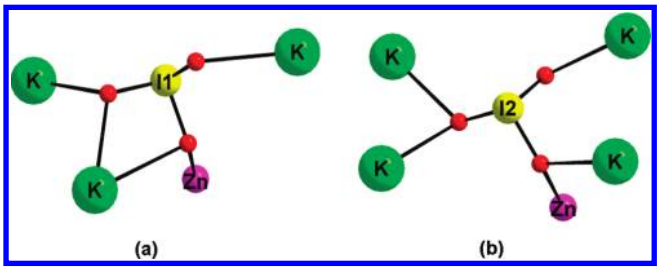

Figure 3. Coordination modes of the iodate anions in the zinc compound.

creating a polar material which is confirmed also by SHG measurements, which will be discussed later. The packing of 0D $Zn(IO_3)_4(H_2O)_2^{2-}$ anions also results in the formation of 1D pseudo tunnels of 8-member rings along *b*-axis which are filled by K^+ ions (Figure 2b). In connectivity terms, the structure maybe written as $\{[Zn_{4/2}O_{2/1}]^{2+}\ 4[IO_{2/1}O_{1/2}]^-\}^{2-}$, with charge balanced by two K^+ cations.

The two IO_3^{2-} groups display different coordination fashions (Figure 3). The $I(1)O_3^{2-}$ anion is pentadentate; it chelates bidentately with one K(2) ion and also bridges to K(1) and Zn ions with two different O atoms, another O atom is bonded with two K ions (Figure 3a). The $I(2)O_3^{2-}$ anion is also pentadentate, one O atom bridges to K(1) and Zn ions, one O atoms bridges to two K ions, and the last one is only connected to one K ion (Figure 3b).

It is noticed that the cell volumes of the four compounds have the following trend: Mn > Mg > Zn > Co, as are most of M−O and K−O bond distances, but the differences are very small. These differences could be generally explained by the different radii for the divalent metal centers. The Pauling ionic radii for the six-coordinated divalent metal ions are 0.80, 0.74, 0.72, and 0.65 Å, respectively, for Mn^{2+}, Zn^{2+}, Co^{2+}, and Mg^{2+}.[29]

The IR spectra of the four compounds display absorption bands associated with the aqua ligands at 3083−3006 cm^{-1}.[13] The characteristic bands of the iodate anions in four compounds appeared at around 801−802 (ν_1), 756−783 (ν_2), 721−722 (ν_3) cm^{-1} (see Supporting Information, Figure S3).[13]

(29) (a) Pauling, L. *The Nature of the Chemical Bond*, 3rd ed.; Cornell University Press: Ithaca, NY, 1960. (b) Shannon, R. D. *Acta Crystallogr.* **1976**, *A32*, 751.

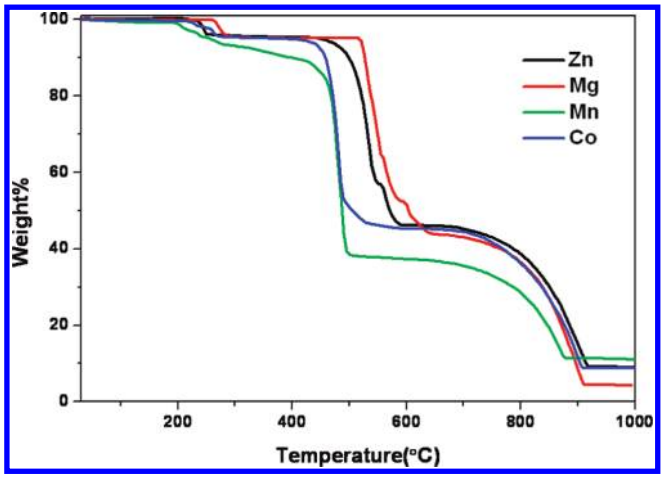

Figure 4. TGA diagrams for $K_2M(IO_3)_4(H_2O)_2$ (M = Mn, Co, Zn, Mg).

All four compounds are moisture and air stable at room temperature. TGA analyses under a nitrogen atmosphere indicate that the four compounds are stable up to 200 °C (Figure 4). Then, all of them exhibit three main steps of weight losses (200−315 °C, 315−664 °C, and 664−918 °C). The first one corresponds to the release of two aqua ligands, and the observed weight losses are 4.15%, 4.05%, 4.0%, and 4.38% for the Mn, Co, Zn, and Mg compounds, respectively, which are close to the calculated ones (4.3% for **Mn**; 4.2% for **Co**; 3.9% for **Zn**; 4.6% for **Mg**). The second and the third one overlapped, during which the iodate anions are decomposed to I_2 and O_2. The total weight losses at 968 °C are 11.38%, 8.8%, 9.0%, and 4.46% for the Mn, Co, Zn, and Mg compounds, respectively. The observed weight losses are close to the calculated ones (10.01% for **Mn**; 8.53 for **Co**; 8.9% for **Zn**; 4.47% for **Mg**) if we assume the final residuals are metal oxides. The final residues were not characterized because of their melting with the TGA bucket made of Al_2O_3 under such high temperature; however, they are expected to be mainly a mixture of metal oxides.

Optical diffuse reflectance spectrum studies indicate that $K_2M(IO_3)_4(H_2O)_2$ (M = Mn, Co, Zn, Mg) revealed optical band gaps of 3.4, 3.5, 4.35, and 4.37 eV, respectively, for the Mn, Co, Zn and Mg compounds (Supporting Information,

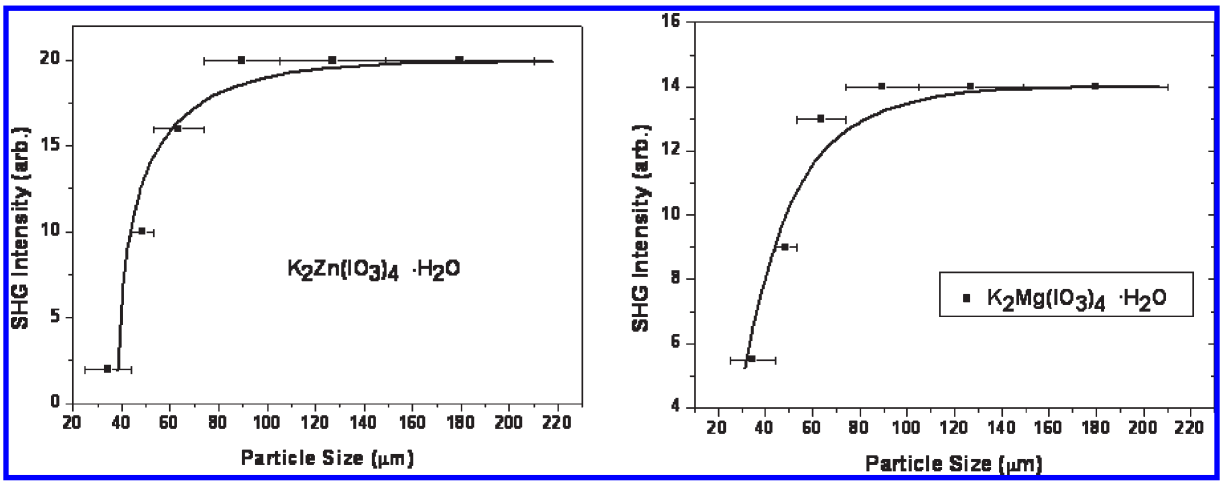

Figure 5. Phase matching curve (particle size) versus SHG intensity for the Zn and Mg compounds.

Figure S4). The differences of the band gaps for these isostructural compounds are mainly because of different electronic configurations for the divalent metal(II) cations. The UV spectrum for Zn and Mg compounds display the characteristic absorption bands in the range of about 1500−2400 nm which may correspond to the presence of water molecules (Supporting Information, Figure S5).

SHG Measurements. $K_2M(IO_3)_4(H_2O)_2$ (M = Mn, Co, Zn, Mg) crystallized in the acentric space group. Hence, it is worthy to study their SHG properties. SHG measurements on a Q-switched Nd: YAG laser with the sieved powder sample (80−100 mesh) revealed that $K_2M(IO_3)_4(H_2O)_2$ (M = Co, Zn, Mg) display SHG signals that are about 0.3, 2.3, and 1.4 times that of KDP, respectively. Because of the absorption of the **Co** compound near 550 nm, its SHG efficiency is much weaker. The SHG signal for the power sample of the **Mn**(II) compound is not detectable. It should be mentioned that the **Mn** and **Co** compounds both have d-d absorptions in the relevant region, and the weak spin-forbidden transitions of **Mn**(II) would not be expected to show up well in diffuse reflectance. We deem that the much weaker SHG responses of **Mn** and **Co** compounds compared with those of **Zn** and **Mg** compounds are also related to the existence of the significant racemic twinning components in both compounds, which will cancel part of the polarization of the iodate groups. Furthermore, the **Zn** and **Mg** compounds were found to be phase-matchable (Figure 5). Phase-matchable experiments for the **Co** compound were not performed since its SHG response is insignificant. On the basis of structural data, it is expected that the polarization contributions of the $I(2)O_3^-$ groups are small since their dipole moments are mainly aligned in opposite directions and almost cancel each other. The main polarization contributions are from $I(1)O_3^-$ groups since their dipole moments are aligned in the same directions (along the *b* axis) as mentioned earlier.

Theoretical Studies. To further understand the chemical bonding and the optical properties of these compounds, $K_2Zn(IO_3)_4(H_2O)_2$ and $K_2Mg(IO_3)_4(H_2O)_2$ were selected as two representatives to calculate their band structures, density of states (DOS) as well as linear and second-order optical properties.

The calculated band structures of $K_2Zn(IO_3)_4(H_2O)_2$ and $K_2Mg(IO_3)_4(H_2O)_2$ along high symmetry points of the first Brillouin zone are plotted in Figure 5. Isomorphic compounds lead to similar band structures. As shown in Supporting Information, Figure S6, both the top of the VB and the bottom of the CB show a small dispersion for both compounds. Both the lowest energy (2.70 eV for the **Zn** compound and 2.76 eV for the **Mg** compound) of CBs and the highest energy (0.0 eV) of VBs are located at the G point. Hence, the direct band gaps of around 2.70 eV and 2.76 eV respectively for the **Zn** and **Mg** compounds are obtained, which are much smaller than the experimental values (4.35 and 4.37 eV for the **Zn** and **Mg**, respectively). This is not surprising as it is well-known that the GGA does not accurately describe the eigenvalues of the electronic states, which causes quantitative underestimation of band gaps, especially for insulators.[28]

The bands can be assigned according to the total and partial density of states (DOS), as plotted in Supporting Information, Figure S7. For $K_2Zn(IO_3)_4(H_2O)_2$ (Supporting Information, Figure S6a), the CBs just above the Fermi level are mainly derived from I-5s, I-5p, and O-2p states. The VBs from −6.55 eV to the Fermi level are mainly composed of O-2p, I-5p, and Zn-3d states and those from −11.64 ev to −8.9 eV are composed of I-5p, K-3p, and I-5s, mixing with small amount of O-2p, O-2s, and H-1s states. O-2s and I-5s states dominate the energy region between −21 and −16.4 eV, and the lowest VBs arise from I-5s and K-3s states. For $K_2Mg(IO_3)_4(H_2O)_2$ (Supporting Information, Figure S6b), the bands above the Fermi level are derived from I-5p, I-5s, and O-2p, mixing with small amount of K-4s, K-4p and Mg-3s, Mg-3p states. The VB from −6.11 eV to the Fermi level are mainly composed of O-2p and I-5p states, and the K-3p, I-5p, some O-2p, I-5s, and H-1s states dominate the VBs ranging from −8.8 to −11.43 eV. In addition, the VBs between −17.7 and −21.5 eV are mainly contributions from the O-2s, I-5s, and small H-1s states, and the lowest VBs are composed of K-3s and I-5s states.

Population analyses allow for a more quantitative bond analysis. The calculated bond orders of Zn−O, K−O, and I−O bonds are 0.20−0.27, 0.09−0.14, and 0.24−0.44 e, respectively, for $K_2Zn(IO_3)_4(H_2O)_2$. For $K_2Mg(IO_3)_4(H_2O)_2$, the calculated bond orders of Mg−O, K−O, and I−O bonds are 0.14−0.28, 0.10−0.13, and 0.24−0.44 e, respectively. Hence, it is concluded that

Zn−O and Mg−O bonds have more covalent character than K−O bonds.

The linear optical response properties of $K_2Zn(IO_3)_4(H_2O)_2$ and $K_2Mg(IO_3)_4(H_2O)_2$ were examined through calculating the complex dielectric function $\varepsilon(\omega) = \varepsilon_1(\omega) + i\varepsilon_2(\omega)$. The imaginary part ($\varepsilon_2(\omega)$) can be used to describe the real transitions between the occupied and unoccupied electronic states. The imaginary parts of the frequency-dependent dielectric function of $K_2Zn(IO_3)_4(H_2O)_2$ and $K_2Mg(IO_3)_4(H_2O)_2$ show anisotropy along the principal dielectric axis directions (See Supporting Information, Figure S8). The curves of the averaged imaginary part and real part of dielectric function were obtained by $\varepsilon^{ave} = (\varepsilon_x + \varepsilon_y + \varepsilon_z)/3$, as displayed in Supporting Information, Figure S9 for the **Zn** and **Mg** compounds, respectively. It is found that the strongest adsorption peaks for the two compounds are very close to each other, located at about 6.45 eV, which can be mainly assigned to the electronic interband transitions from the O-2p to I-5p states. The average static dielectric constants $\varepsilon(0)$ are 3.46 and 3.35 for the **Zn** and **Mg** compounds, respectively. The dispersion of refractive index, which was calculated by the formula $n^2(\omega) = \varepsilon(\omega)$, indicating the orders of $n^x > n^y \geq n^z$ and $n^x > n^y > n^z$ for the **Zn** and **Mg** compounds, respectively (Supporting Information, Figure S10). For the **Zn** compound, the n^x, n^y, and n^z values at 1064 nm are 1.886, 1.869, and 1.868, respectively, and the corresponding values are1.854, 1.841, and 1.833 for the **Mg** compound.

The space group of the isostructural $K_2Zn(IO_3)_4(H_2O)_2$ and $K_2Mg(IO_3)_4(H_2O)_2$ crystals belongs to class *2* and has 8 non-vanishing tensors of second-order susceptibilities. Under the restriction of Kleinman's symmetry, only four independent SHG coefficient tensors (d_{14}, d_{21}, d_{22} and d_{23}) are left. The frequency-dependent SHG tensors of the **Zn** and **Mg** compounds are plotted in Supporting Information, Figure S11. The values of d_{14}, d_{21}, d_{22}, and d_{23} at the wavelength of 1064 nm (1.165 eV) for the **Zn** compound are 1.83×10^{-9}, 2.18×10^{-9}, 5.83×10^{-9}, and 3.66×10^{-9} esu, respectively, and the corresponding values for the **Mg** compound are 1.91×10^{-9}, 2.62×10^{-9}, 5.19×10^{-9}, and 4.06×10^{-9} esu. These values are somehow higher than our experimental values, which are 2.3 and 1.4 times of that of KDP ($d_{36} = 1.1 \times 10^{-9}$ esu) for the **Zn** and **Mg** compounds, respectively, which is probably mainly due to the limitations of the calculation methods as well as the fact that the calculations are based on single crystals rather than powder samples.

In summary, four novel mixed metal iodates, namely, $K_2M(IO_3)_4(H_2O)_2$ (M = Mn, Co, Zn, Mg) have been successfully isolated and structurally characterized. They are isomorphous, and their structures feature 0D $\{M(IO_3)_4(H_2O)_2\}^{2-}$ anions in which the M(II) centers are octahedrally coordinated by two *trans*-aqua ligands and four monodentate iodate anions; these 0D $\{M(IO_3)_4(H_2O)_2\}^{2-}$ anions are separated by K^+ cations. The **Zn** and **Mg** compounds display moderate strong SHG response whereas the SHG signal for the **Co** compound is very weak and that of the **Mn** compound is not detectable. We deem that this is mainly due to different electronic configurations for the divalent metal ions which have strong effects on the interband transitions and the colors of the compounds, as well as on the racemic twinning problem. Our future research efforts will be devoted to grow large size single crystals of $K_2M(IO_3)_4(H_2O)_2$ (M = Zn, Mg) to further study their optical properties, such as refractive index, the Sellmeier equations, second-order NLO coefficients, and the laser damage threshold.

Acknowledgment. This work was supported by the National Natural Science Foundation of China (20731006, 20825104, and 20821061), Key Project of FJIRSM (No. SZD09001), Key Project of Chinese Academy of Sciences (No. KJCX2-YW-H01) and NSF of Fujian Province (No. E0420003).

Supporting Information Available: IR spectra, simulated and experimental XRD powder patterns for $K_2M(IO_3)_4(H_2O)_2$ (M = Mn, Co, Zn, Mg). CSD reference numbers 421244, 421243, 421242, and 421245. This material is available free of charge via the Internet at http://pubs.acs.org.